Dependence of DNA Electronic Structure on Environmental and Structural Variations

J. B. MacNaughton* and A. Moewes

Department of Physics and Engineering Physics, University of Saskatchewan, 116 Science Place, Saskatoon, Saskatchewan S7N 5E2, Canada

J. S. Lee

Department of Biochemistry, University of Saskatchewan, 107 Wiggins Road, Saskatoon, Saskatchewan S7N 5E5, Canada

S. D. Wettig

College of Pharmacy and Nutrition, University of Saskatchewan, 110 Science Place, Saskatoon, Saskatchewan S7N 5C9, Canada

H.-B. Kraatz

Department of Chemistry, University of Saskatchewan, 110 Science Place, Saskatoon, Saskatchewan S7N 5C9, Canada

L. Z. Ouyang

Department of Physics and Mathematics, Tennessee State University, 3500 John A. Merritt Boulevard, Nashville, Tennessee 37209

W. Y. Ching

Department of Physics, University of Missouri−Kansas City, 5100 Rockhill Road, Kansas City, Missouri 64110

E. Z. Kurmaev

Institute of Metal Physics, Russian Academy of Sciences Ural Division, 620219 Yekaterinburg GSP-170, Russia

Received: April 24, 2006; In Final Form: June 9, 2006

We present experimental and theoretical evidence that varying the local environment and physical structure of dried DNA has a direct impact on its electronic structure. By preparing samples of DNA in various solutions, it was possible to alter the type of ions present during the production of the DNA samples. These variations resulted in differences in the local chemical environment of the dried DNA molecules. X-ray absorption spectroscopy (XAS) and X-ray emission spectroscopy (XES) were used to probe the variations in the electronic structure of DNA samples. DFT calculations of a stack of 10 adenine (A)−thymine (T) nucleobase pairs show that slight structural variations in stacking height have a direct influence on the electronic structure and result in changes to the HOMO−LUMO gap. The effects of these differences in the local environment on the electronic structure are discussed and are related to the results of conductivity measurements of DNA.

Introduction

The possibility of using DNA as a molecular nanowire has encouraged extensive research into the conductive properties of the molecule. What is the conductivity of DNA? Can it be determined whether it is conducting, insulating, or in the semiconducting regime? It seems that these questions are similar to inquiring about the conductive nature of doped silicon. Like those materials, numerous variations of DNA exist, and the conductivity is specific to the individual system with the impurities playing the key role. In the case of semiconductors, the importance of impurities is well-known, while questions concerning similar effects in DNA are only now emerging. We therefore suggest that there is little relevance in trying to determine the exact value of the conductivity of DNA in general; if this property is to be examined, it must be analyzed on a case-by-case basis.

Considerable discussion regarding the conductivity of DNA exists in the literature, and conflicting results have reported insulating,[1−4] semiconducting,[5−7] highly conductive,[8] or superconducting[9] behavior for the DNA molecule. Many of the attempts to analyze the conductivity have been microscopic, involving the stretching of a DNA strand between two electrodes[1−3,5−9] and the measuring of current−voltage ($I-V$) characteristics. While these techniques provide information for that specific arrangement, a more general understanding of the macroscopic behavior would be beneficial. Unlike previous studies involving a microscopic method of measuring $I-V$

* Corresponding author. Tel.: +306-966-6380; fax: +306-966-6400; e-mail: Janay.m@usask.ca.

10.1021/jp062516w CCC: $33.50
Published on Web 07/22/2006

curves, we have used a spectroscopic and macroscopic approach. Examining the electronic structure with soft X-ray absorption (XAS) and emission (XES) spectroscopy using synchrotron radiation provides valuable information about the occupied and unoccupied partial densities of states without the requirement of a microscopic setup.

DNA is a right-handed helical stack of complementary pairs of nitrogen-containing bases supported by a backbone consisting of a deoxyribose (sugar)−phosphate sequence. A negative charge is associated with the phosphate groups in the backbone of the helical structure. This negatively charged backbone attracts cations. It is understood that the structure of DNA in solution is sensitive to hydration and ions. It is found that the dominant effects on conformational stability of the molecule come from a balance of competing factors involved in the electrostatic free energy, including the phosphate repulsions internal to the DNA, the electrostatic component of hydration, and the electrostatic effects resulting from the cations.[10] Results from a recent theoretical molecular dynamics study modeling the behavior of Na^+ and K^+ have shown that the choice of a monovalent ion determines the location of binding sites on the DNA helix and can result in slight differences in the DNA structure.[11]

The cations that surround the helix to counterbalance the net negative charge on the phosphate backbone will influence many properties of DNA in the solid state.[12] During the transition of DNA from a solution into the solid state, cations and water molecules remain incorporated in the local environment of the DNA structure. Several known phases of DNA exist, including two right-handed helix formations. These include B-DNA, which is the most common well-known structural form and is stabilized under conditions of high water content, and A-DNA, which is favored under lower water content conditions.[10] Either A-DNA or a combination of A- and B-DNA may be favorable in dry DNA because of the lower water content constraint. There are specific differences between the structures of the different forms of DNA: in B-DNA, the base pairs have an average separation of 3.4 Å and a relative twist angle of 36°, while A-DNA has a base pair separation and twist angle of 2.5 Å and 32.7°, respectively.[13] The concentration and size of cations are important in instigating phase transitions in DNA.[12] By varying the type of cation in the structure of DNA, the energy values for both the highest occupied molecular orbital (HOMO) and the lowest unoccupied molecular orbital (LUMO) are altered.[14] Specifically, the type of cation and its distribution in the structure can influence such macroscopic properties as conductivity.[4,13−16]

X-ray absorption spectra and X-ray emission spectra have been measured and subsequently used to determine changes in the experimental HOMO−LUMO energy gap. These values have been used to demonstrate differences in the electronic structure of DNA samples prepared with various solutions. Recent calculations based on density functional theory (DFT) reveal that the HOMO and LUMO are π and π^* orbitals, respectively, that are associated with the nucleobases in the DNA structure.[2] Therefore, the nitrogen partial density of electronic states has been examined experimentally and theoretically to probe the effects of a varying local environment on the HOMO−LUMO energy gap. This is appropriate because the nitrogen atoms in the DNA structure are located exclusively in the nucleobases. Our DFT calculations further indicate that slight structural changes, achievable by altering the local environment of the DNA molecule, can have an influence on both the electronic structure and the conductivity of DNA.

Sample Synthesis

Calf thymus DNA (42% G−C, 58% A−T) was purchased from Sigma. The DNA samples were prepared by lyophilization of 25 mL of 100 μg/mL calf thymus DNA prepared in the appropriate solution. The solutions used for the preparation were tris(hydroxymethyl)aminomethane (TRIS) buffer (pH 7.5), potassium phosphate buffer (pH 7.5), boric acid buffer (pH 8.6), and a sodium chloride solution (pH 6.8). All buffer/salt concentrations were 10 mM. All samples of DNA were prepared in solution, then dried and measured in powder form. Three full sets of samples were synthesized using the same procedure and used in this study (sample sets #1−3).

The DNA samples were prepared in various solutions, ensuring a unique ionic (both cation and anion) environment during the preparation and subsequent drying of the samples. The method used for sample preparation in this study had two main objectives. The first was to vary the identity of ions present during the drying of the samples by changing the solution. For the TRIS buffer, the main cations consisted of H^+ and $NH(CH_2OH)_3)^+$, while the anion was Cl^- resulting from pH adjustments using HCl. Boric acid contributed H^+, Na^+, $H_2BO_3^-$, and OH^- (from pH adjustments using NaOH). The cation from potassium phosphate was K^+, the anions were a mixture of both $KH_2PO_4^-$ and $K_2HPO_4^{2-}$, and NaCl contributed Na^+ and Cl^-. Electrostatic concepts determine that the negative charge of the DNA backbone will attract the cations to its structure, in addition to water molecules that remain in the structure after the drying process. This process produces a compound of $[(DNA)^{n-} \bullet nA^+ \bullet mH_2O]$, where n is the number of negative phosphate groups, A is the cation, and m is the number of water molecules. The second main objective was to repeat the same sample preparation to show that even when the synthesis conditions are the same, the DNA powders produced will not be identical to those previously synthesized. Although conditions can be controlled while in solution form and the method of drying the samples can be repeated, the samples will always contain variations.

Modifications to the final dried DNA sample can occur during the drying process as a result of four main categories of factors: (1) cation distribution around the helix, (2) water molecule distribution around the helix, (3) structural changes in the DNA molecule, and (4) solid-state variations due to formations of bundles or other solid-state type structures. These four categories are interrelated; for example, differences in the water molecule distribution around the helix can change the structure of DNA.[13] During the drying process, the DNA structure will attempt to minimize its total energy; it is clear, however, that many energy minima will exist. This ensures a wide assortment of variations in the four categories, and understanding how these deviations affect the properties of the dried DNA molecule is essential.

Experimental Procedures

The soft X-ray spectroscopic measurements were performed at Beamline 8.0.1 at the Advanced Light Source (ALS) located at the Lawrence Berkeley National Laboratory. The X-ray absorption spectra presented in this study were measured in total electron yield (TEY) mode. The resolving power $E/\Delta E$ for the absorption spectra is about 5000 at the nitrogen edge. For the emission spectra, the emitted radiation is partially collected in a Rowland circle-type spectrometer with spherical gratings and recorded with an area-sensitive multichannel detector. The details of this endstation are described elsewhere.[17] Total experimental resolution in the N Kα X-ray emission region is

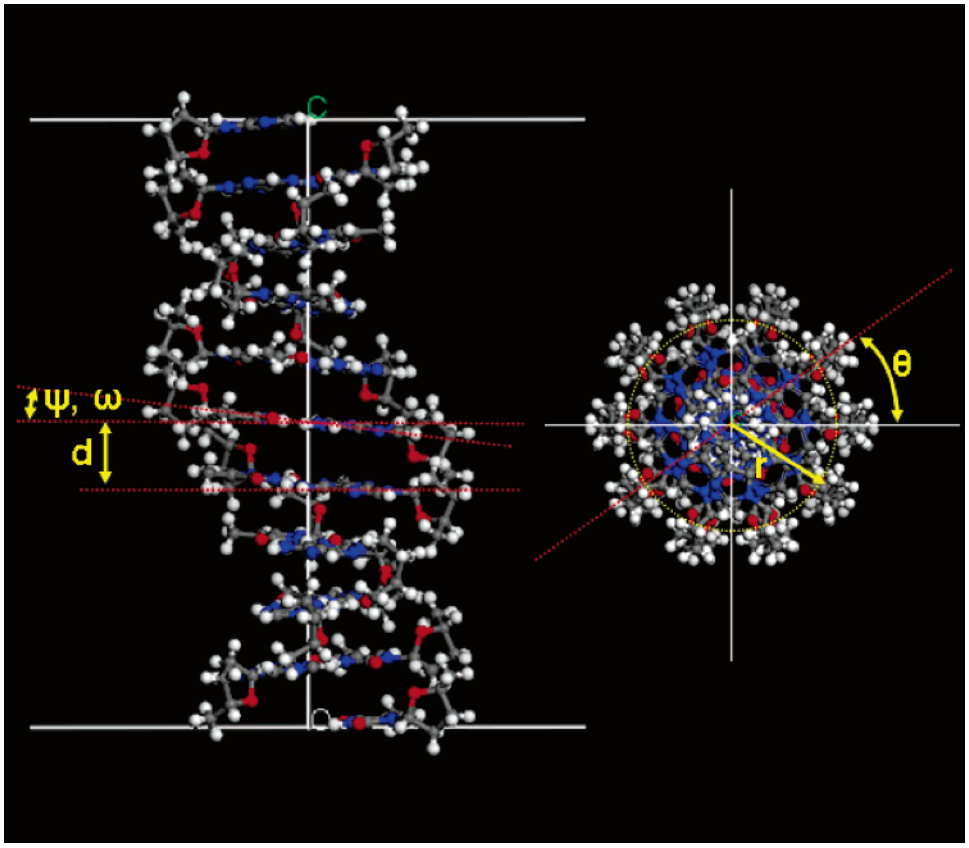

Figure 1. Ball-and-stick depiction of the periodic 10 A−T base pair DNA model for the *x*-axis (left) and *z*-axis (right). For the diagram, *d* is the stack height, *r* is the helix radius, θ is the twist angle, and (ψ, ω) are the tilt/roll angles.

0.75 eV fwhm. All absorption and emission spectra are normalized to the number of photons falling on the sample, monitored by a highly transparent gold mesh in front of the sample. The experimental procedure was designed to minimize radiation damage to the samples during measurements. Radiation damage was reduced by minimizing the exposure time and the photon flux and maximizing thermal conductivity for the sample. Radiation damage is a greater concern in XES measurements than in XAS, due to the larger radiation dose that is required. However, as the variation in the XES spectra was relatively small as compared to that observed in the XAS spectra, we feel confident in our assumption that radiation damage had little to no effect on our findings.

Soft X-ray spectroscopic techniques were used to study the three different batches of DNA samples, synthesized using the same procedure but at different times (sample sets 1−3). Over the time period of 1 week, spectra were measured from five different sample plates prepared from DNA powders taken from sample set #1 (trials 1−5). Spectra were measured on one occasion from sample set #2 (trial 6) and once from sample set #3 (trial 7).

Calculations

To complement the experimental measurements, ab initio density functional calculations of the electronic structure of a model of DNA were completed. To clarify that the choice of solution can affect DNA physical structure and hence electronic structure, we built a series of periodic DNA stacking models with 10 adenine (A)−thymine (T) nucleobase pairs to simulate the effects of solvents (Figure 1). The double helix DNA structure can be described by six parameters: *x*−*y* plane shifts perpendicular to the helix axis, stacking height, twist angle, and tilt/roll angles. The periodic constraint reduces the number of free parameters. For a periodic stack of 10 A−T nucleobase pairs, the twist angle is 36° and the *x*−*y* plane shift reduces to one helix radius. The stacking height, helix radius, and tilt/roll angles are all influenced by the solvent through weak electrostatic interactions. The variations in stacking heights, helix radius, and tilt/roll angles affect the electron overlap between adjacent nucleobases and, therefore, the HOMO−LUMO energy gap. Seven structural models of periodic stacks of 10 A−T base pairs with stacking heights ranging from 3.38, 3.28, 2.98, 2.78, 2.58, 2.38, and 2.18 Å were generated and relaxed using the Amber program.[18] To isolate the effect on the energy gap due to structural changes of nucleobase moieties, we have removed the PO_4 group from our models and subsequently terminated the resulting broken bonds with hydrogen atoms. The dimension of the unit cell was set to 20 Å × 20 Å (10 times stacking height) to minimize the interaction between neighboring DNA chains. A total of 580 atoms $(C_{10}N_5OH_{13}{\bullet}C_{10}N_2O_3H_{14})_{10}$ made up each unit cell.

The electronic structure of the periodic DNA models was calculated using the orthogonal linear combination of the atomic orbitals (OLCAO) method[19,20] within the local approximation of the density functional theory. The OLCAO method employs Bloch sums of atomic orbitals represented by atom-centered Gaussian functions as the basis functions and are more compact and computationally efficient than the plane wave-based methods. The method is particularly efficient for materials with complex structures and low symmetry and has been successfully applied to complex vitamin B_{12} molecules.[21−24] In the present calculations, we employed a basis set consisting of atomic orbitals of C, N, O (1s,2s,2p,3s,3p), and H (1s,2s,2p). More than 50 iterations were needed to have a fully converged self-

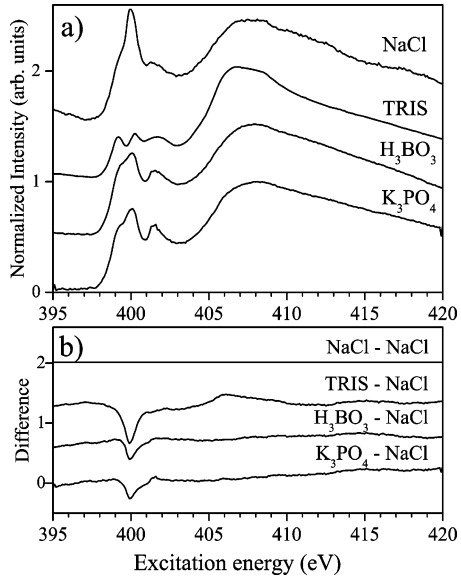

Figure 2. (a) Experimental nitrogen 1s XAS for DNA prepared with TRIS buffer, potassium phosphate buffer, boric acid buffer, and a NaCl solution. (b) Difference spectra found by subtracting the spectrum of DNA (NaCl) from each of the spectra in panel a. An offset for the *y*-axis has been added for clarity.

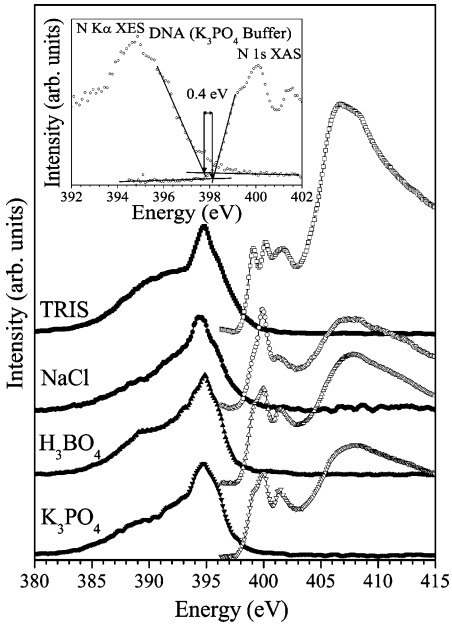

Figure 3. Nitrogen edge XES and XAS spectra for DNA prepared in various solutions. An offset for the *y*-axis has been added for clarity. The inset displays the N 1s XAS and XES spectra of potassium phosphate buffer used for demonstration of experimental HOMO−LUMO gap measurements.

consistent potential with the energy eigenvalues stabilized to within 0.01 meV. The solution of the secular equation provides the energy eigenvalues for the model from which the density of states (DOS) can be obtained. A special advantage of the OLCAO method is the ability to resolve the DOS into atom-specific partial DOS (PDOS) to facilitate interpretation of experimental data. In the present work, the most relevant data is the nitrogen PDOS, which can be related to the XAS and XES measurements described in the Experimental Procedures.

Results and Discussion

Figure 2a shows the nitrogen 1s X-ray absorption spectra of the DNA samples prepared with tris(hydroxymethyl)aminomethane (TRIS) buffer (pH 7.5), potassium phosphate buffer (pH 7.5), boric acid buffer (pH 8.6), and a sodium chloride solution (pH 6.8). These spectra were obtained in trial 7, measured from DNA samples from sample set #3. X-ray absorption spectra probe the partial unoccupied local electronic density of states, and these spectra clearly demonstrate differences between the various DNA powders prepared with different solutions. The lower energy features following the absorption onset are the result of excitations to π^* type orbitals, while the broader features located at higher energy are produced from exciting the nitrogen 1s electron to σ^* orbitals. Previous spectral results have shown this sensitivity to chemical environment,[25] and the exact transitions have been determined for the nitrogen XAS spectra of the nucleobases.[26] One of the clear differences in the spectra is the enhancement of the lowest energy π^* feature (399.1 eV) in the DNA spectra prepared with TRIS buffer. Since the TRIS buffer contains nitrogen atoms, DNA and the buffer influence this spectrum, and it is not possible to distinguish contributions from buffer and DNA where the buffer contains nitrogen atoms.

From each spectrum in Figure 2a, the NaCl spectrum has been subtracted, and the difference spectra are shown in Figure 2b. The spectrum of DNA produced in a salt solution was subtracted because it is considered to be the solution containing the most simple ion arrangement. This plot illustrates that the main differences in the spectra occur near the onset region, in the excitations to the π^* orbitals (LUMO). In this preedge region, the DNA prepared with NaCl has a greater intensity in the π^* transition at 400 eV as compared to the other spectra, therefore causing the difference spectra to be negative for part of this region. It is shown that the XAS spectra are sensitive to slight modifications of the electronic structure that result from the unique cation environments instigated by sample preparation using different solutions.

Figure 3 displays the combination of XES and XAS spectra for the samples measured in trial 7 giving a complete picture of the partial density of states at the nitrogen edge of the four DNA samples. The electronic structure in the regions of the HOMO and LUMO affects a material's conductivity. Several charge-transfer mechanisms have been proposed for microscopic samples of DNA, including superexchange, incoherent hopping, or band-like transport as described in a recent review of DNA's conductivity[13] or a more specific review of charge-transfer studies of biomolecules.[27] Regardless of which electron-transfer mechanism is applicable, all of the methods have a dependence on the arrangement of electrons in the molecule. Using the spectroscopic techniques as a probe of this electronic structure, a comparison between four samples is made in Figure 3. The same XAS spectra from Figure 2 are displayed with the corresponding XES spectra. Although the most obvious variations between spectra occur in the preedge features of the XAS spectra, slight differences are seen in the high energy slope of the XES spectra and the lower energy region around 390 eV. An increase in the HOMO−LUMO gap is found from the top to the bottom sets of the XES and XAS spectra.

By combining XES and XAS experimental data onto a single energy axis, it is possible to estimate a HOMO−LUMO energy gap measurement.[26,28−30] Experimental results are made comparable by carefully calibrating the energy axes of spectra from the various trials with known spectral peak locations of hexagonal boron nitride (*h*-BN).[31] The standard sample of *h*-BN pressed powder was measured during every trial to guarantee that consistent calibration could be achieved and to ensure that any differences in the DNA energy gaps were the result of

variations in the samples, not due to changes in monochromator photon energies. It is important to note that the absolute gap values are only as certain as the calibration values taken from the study of hexagonal boron nitride by Fomichev and Rumsh.[31]

The procedure for determining the energy gap is displayed in the inset in Figure 3 for a DNA sample prepared with a potassium phosphate buffer solution. Lines are extended along the spectral slope, and the intersections with the background levels are located. The linear extrapolation method was applied to remove the tail in the spectra caused by instrumental (Gaussian) and lifetime (Lorentzian) broadening. The down slope of the emission spectrum was used to determine the first intersection (HOMO), and the onset slope of the first π^* feature in the absorption spectrum was used for the second intersection (LUMO). The HOMO−LUMO gap value is given by the energy difference between the two intersections. This is a relatively uncomplicated procedure and is easily reproduced, ensuring that the error in the method is no more than 0.1 eV for each of the boundaries, or ±0.2 eV for the total experimental gap value. It is found that more refined methods for determining the HOMO and LUMO gap boundaries, for example, using the second derivative to determine the inflection points in the onsets of the spectra, do not significantly improve this systematic error.

It is important to note that while this experimental method provides a means for reliably and accurately comparing HOMO−LUMO gaps, it is not simple to determine an absolute value of the gap for a number of reasons. Both the presence of the core hole and the energy calibration to a reference sample have effects on the final results. Core hole effects can cause the onset of the absorption spectrum to shift to a lower energy. The creation of the core hole tends to shift the emission spectrum to lower energy as well, but this effect is minimal due to the final state rule. Results from calculations involved in our previous study on the nucleobases[26] indicate that the inclusion of the nitrogen core hole reduces the HOMO−LUMO gap by a maximum of 0.3 eV in the case of thymine. It is assumed that this shift would be comparable to the case for the DNA molecule. Calibrating the energy axes shifts both emission and absorption data according to measurements performed on a reference sample. To account for unavoidable variations in the optical alignment of the monochromator and spectrometer gratings, this step is necessary to correct the experimental energy scale and to make all measurements comparable but is only as precise as the known values for the peaks in the reference spectra. These both can have direct influence on the experimental gap measurement and are expected to add a larger error to the ±0.2 eV that was outlined previously. This additional error will affect the absolute value of each gap in the same way, but it does not influence the trends when comparing the spectra.

Results from several sets of measurements have been used to determine experimental HOMO−LUMO energy gaps to compare the electronic structure of the DNA samples with different cations incorporated into the local environment. DNA samples taken from sample set #1 were measured five times over the period of 1 week to investigate inconsistencies in the local environments from one particular sample set, as well as possible aging effects. Sample sets #2 and #3 were measured one time each to compare results from newly synthesized sets of samples. Figure 4a displays N 1s XAS results from sample set #1 (trials 1−5), sample set #2 (trial 6), and sample set #3 (trial 7) for DNA prepared with NaCl solution. Figure 4b shows a comparison of nitrogen edge XES and XAS spectra for the DNA sample prepared with NaCl solution and the corresponding

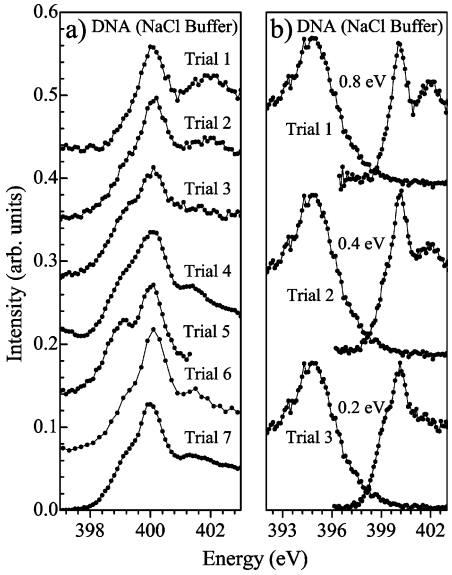

Figure 4. (a) Experimental nitrogen 1s XAS for DNA prepared with a NaCl solution for sample set #1 (trials 1−5), sample set #2 (trial 6), and sample set #3 (trial 7). (b) Experimental nitrogen XAS and XES spectra of DNA prepared with a NaCl solution displaying an experimental HOMO−LUMO gap for three measurements (trials 1−3) from sample set #1. An offset for the *y*-axis has been added for clarity.

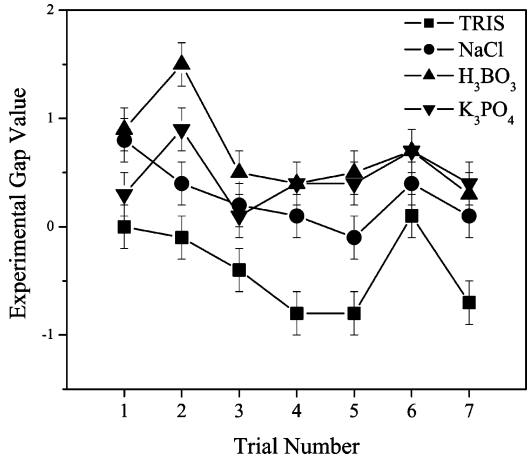

Figure 5. Experimental HOMO−LUMO gap values for DNA prepared with different solutions for seven different trials. The error bars reflect the systematic error resulting from our method of determining the gap using the calibrated measurements.

energy gap measurements determined using the method presented in this study.

In all instances, the gap is found to vary, and the trends are displayed in Figure 5. The error bars reflect the systematic error of ±0.2 eV of our method. Note that the differences in the gap measurements are important in this assessment, not the absolute values, as the experimental gap values depend strongly on factors such as the absolute energy calibration, as was described previously. These experimental measurements can be used in the comparison of the electronic structure between the samples because all data were treated in exactly the same way. For comparison purposes, the values determined from the experimental HOMO−LUMO gap measurements have been given in Table 1. A negative value simply means that there was overlap between the XES and the XAS spectra, as a result of the effects described previously. The overall gap difference from the smallest value to the largest value during each trial is found to vary from 0.6 to 1.6 eV and hence is a much larger energy difference than the systematic error. Differences in the energy

TABLE 1: Experimental HOMO−LUMO Gap Values from DNA Samples

	experimental gap value (eV)						
	sample set 1					sample set 2	sample set 3
	trial 1	trial 2	trial 3	trial 4	trial 5	trial 6	trial 7
TRIS	0	−0.1	−0.4	−0.8	−0.8	0.1	−0.7
NaCl	0.8	0.4	0.2	0.1	−0.1	0.4	0.1
H_3BO_3	0.9	1.5	0.5	0.4	0.5	0.7	0.3
K_3PO_4	0.3	0.9	0.1	0.4	0.4	0.7	0.4
difference[a]	0.9	1.6	0.9	1.2	1.3	0.6	1.1

[a] Difference between largest and smallest gap value for the given trial.

gaps can result from an energy shift of the electronic states, or the creation of new electronic states, or a combination of the two. Both an energy shift in electronic states and the creation of new states has been shown to occur for the relatively simple Si_{46} system when the environment was altered by the addition of Na_8 or K_8 impurities.[32] It is clear that the energy gaps of the DNA samples measured in each of the trials fluctuate, resulting from changes in electronic structure created from variations in the four main categories, previously described as cation distribution, water distribution, structural changes in the DNA molecule, and possible solid-state variations resulting from interactions between the DNA molecules in powder form.

Figure 5 displays that diverse gap values have been found for the four DNA samples in each of the seven trials, resulting from the different cations and anions present during sample preparation. Variations between the values obtained in trials 1−5 are possibly the result of inconsistencies in the local environment of the five samples obtained from sample set #1, but more likely it is an aging effect. Since each of the five sample plates was prepared from the same batch (sample set #1), it is possible that the differences are a result of the DNA samples changing over the week since the energy gap value for each of the four DNA samples follows a similar trend for the first five trials, as shown in Figure 5. This trend is further evidence of the sensitivity of DNA to its environment. The gap values change again for the measurements of sample sets #2 and #3 in trials 6 and 7, respectively, and this change results from differences in the local chemical environment between the three sample sets. Although many factors such as pH, temperature, and drying time are controlled during sample preparation, it is nearly impossible to control the drying process completely. This causes variations in the cation distribution in the dried structure of DNA and differences in the local chemical environment of the samples in the different sample sets. The gap changes because of fundamental dissimilarities in the samples that result from variations in the water and cation environment and possibly from differences in the structure of the DNA samples, such as slight changes in the stacking height as a result of the changes in the chemical environment.

Calculations for the DNA molecule are challenging due to the large unit cell required to accurately represent the molecule. Models need to be simplified from the actual DNA molecule to make the calculation possible. For our density functional calculations, we have chosen a simplified model of DNA that includes a stack of 10 adenine−thymine (A−T) nucleobase pairs. This model has been used in calculations to demonstrate the effect of structural variations on the electronic structure, and the results are displayed in Figure 6. The figure shows the results from repeating the density of states calculations for various values of the stacking height. The stacking height is the projected distance between neighboring base pairs along the helical axis and is varied to simulate slight structural variations. The smaller range of stacking heights corresponds to an A-DNA

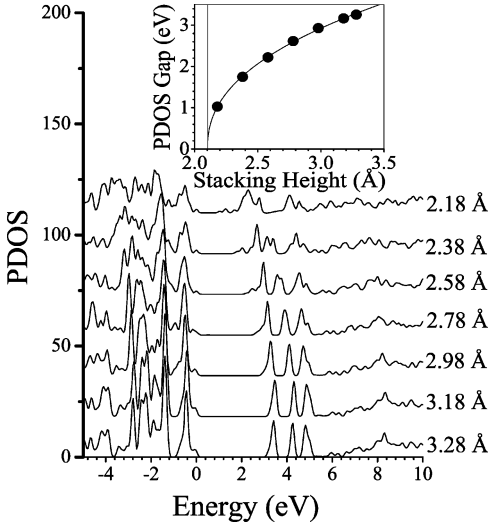

Figure 6. Calculated partial DOS of N atoms for a stack of 10 A−T nucleobase pairs for various values of stacking height using the OLCAO method. An offset for the *y*-axis has been added for clarity. The inset shows that the relationship between the energy gap and the stacking height obeys a power law, $y = A(x - x_c)^P$, where $A = 3.06472$, $x_c = 2.10274$, and $P = 0.42839$. The broadening used for the partial DOS was 0.05 eV (fwhm).

type structure (base pair separation of 2.5 Å), and subsequently, the value is increased to nearly the value for B-DNA (base pair separation of 3.4 Å). As the stacking height increases, the energy gap for the nitrogen states also increases. The theoretical energy gap increases in a predictable way according to a power law, as shown in the inset. The values of the calculated gaps vary from 1.03 to 3.26 eV for the selected range of stacking heights. The gap in the theoretical data was taken to be the difference between the calculated HOMO and the calculated LUMO. A similar trend was found for the value of the energy gap in other DFT calculations, which found an energy gap value of 1.249 eV for the A−T sequence A-DNA and 2.743 eV for the A−T sequence B-DNA.[33] Our calculations clearly show that slight modifications in the physical structure, which can be the direct result of a varying environment of cations and water molecules, will modify the HOMO−LUMO energy gap. This result supports our experimental findings. In the future, it would be possible to include the actual solvent molecules in the calculation, which would act as cations in the local chemical environment of a larger and more realistic DNA model.

Conclusion

X-ray spectroscopy has proven to be extremely sensitive to changes in the environment of the DNA samples, resulting from altering the solution involved with sample preparation. Our X-ray absorption and X-ray emission measurements show that the local chemical environment plays an important role in determining the electronic structure of DNA. Experimental

values of the energy gap provide a means to compare and track changes in the electronic structure of a variety of samples. These modifications in environment and structure can relate to the conductivity. DNA is a complex molecule, subject to extensive variations in hydration and cation distribution, as determined by differences in the electronic structure of the samples used in this study.

Many different results on the conductive nature of DNA have been reported in the literature; however, they all had unique and microscopic experimental setups. The experiment was arranged, and $I-V$ curves were measured, determining a property of the DNA molecule for that one particular setup, in that one particular lab, at that particular time. The conductivity of DNA is highly variable and the question, "what is the conductivity of DNA?" is relatively meaningless in a general sense since it depends strongly on the individual setup. Previous studies used a microscopic approach to measure $I-V$ curves, and we have presented a macroscopic study using spectroscopy. By monitoring the HOMO−LUMO gap directly, we have shown how sensitive the electronic structure of DNA is to variations in chemical environment during sample preparation. This gives a plausible explanation for the many different results that have been measured for the conductivity of DNA; each experiment had different sample preparation, resulting in unique DNA molecules being studied. The challenge will now be to understand how to exert greater control over the interactions of DNA with its surrounding environment in the dried form, such that we could produce a DNA molecule with specific conductive properties in a reproducible way. Knowing how DNA interacts with its local chemical environment is crucial in understanding and tailoring its conductive properties.

Acknowledgment. Funding by the Natural Sciences and Engineering Research Council of Canada (NSERC) is gratefully acknowledged. A.M. and H.-B.K. are Canada Research Chairs. The work at the Advanced Light Source at the Lawrence Berkeley National Laboratory was supported by the U.S. Department of Energy (Contract DE-AC03-76SF00098). The work at UMKC was supported by the U.S. Department of Energy under Grant DE-FG02-84DR45170.

References and Notes

(1) Braun, E.; Eichen, Y.; Sivan, U.; Ben-Yoseph, G. *Nature* **1998**, *391*, 775.

(2) de Pablo, P. J.; Moreno-Herrero, F.; Colchero, J.; Herrero, J. G.; Herrero, P.; Baro, A. M.; Ordejon, P.; Soler, J. M.; Artacho, E. *Phys. Rev. Lett.* **2000**, *85*, 4992.

(3) Storm, A. J.; van Noort, J.; de Vries, S.; Dekker, C. *Appl. Phys. Lett.* **2001**, *79*, 3881.

(4) Tran, P.; Alavi, B.; Gruner, G. *Phys. Rev. Lett.* **2000**, *85*, 1564.

(5) Porath, D.; Bezryadin, A.; de Vries, S.; Dekker, C. *Nature* **2000**, *403*, 635.

(6) Yoo, K. H.; Ha, D. H.; Lee, J. O.; Park, J. W.; Kim, J.; Kim, J. J.; Lee, H. Y.; Kawai, T.; Choi, H. Y. *Phys. Rev. Lett.* **2001**, *87*, 198102.

(7) Rakitin, A.; Aich, P.; Papadopoulos, C.; Kobzar, Y.; Vedeneev, A. S.; Lee, J. S.; Xu, J. M. *Phys. Rev. Lett.* **2001**, *86*, 3670.

(8) Fink, H. W.; Schönenberger, C. *Nature* **1999**, *398*, 407.

(9) Kasumov, A. Y.; Kociak, M.; Gueron, S.; Reulet, B.; Volkov, V. T.; Klinov, D. V.; Bouchiat, H. *Science* **2001**, *291*, 280.

(10) McConnell, K. J.; Beveridge, D. L. *J. Mol. Biol.* **2000**, *304*, 803.

(11) Várnai, P.; Zakrzewska, K. *Nucleic Acids Res.* **2004**, *32*, 4269.

(12) Weidlich, T.; Lindsay, S. M.; Rupprecht, A. *Phys. Rev. Lett.* **1988**, *61*, 1674.

(13) Endres, R. G.; Cox, D. L.; Singh, R. R. P. *Rev. Mod. Phys.* **2004**, *76*, 195.

(14) Adessi, C.; Anantram, M. P. *Appl. Phys. Lett.* **2003**, *82*, 2353.

(15) Adessi, C.; Walch, S.; Anantram, M. P. *Phys. Rev. B* **2003**, *67*, 081405.

(16) Hübsch, A.; Endres, R. G.; Cox, D. L.; Singh, R. R. P. *Phys. Rev. Lett.* **2005**, *94*, 178102.

(17) Jia, J. J.; Callcott, T. A.; Yurkas, J.; Ellis, A. W.; Himpsel, F. J.; Samant, M. G.; Stöhr, J.; Ederer, D. L.; Carlisle, J. A.; Hudson, E. A.; Terminello, L. J.; Shuh, D. K.; Perera, R. C. C. *Rev. Sci. Instrum.* **1995**, *66*, 1394.

(18) Pearlman, D. A.; Case, D. A.; Caldwell, J. W.; Ross, W. S.; Cheatham, T. E.; Debolt, S.; Ferguson, D.; Seibel, G.; Kollman, P. *Comput. Phys. Commun.* **1995**, *91*, 1.

(19) Ching, W. Y. *J. Am. Ceram. Soc.* **1990**, *73*, 3135.

(20) Ching, W. Y. In *The Magnetism of Amorphous Metals and Alloys*; Fernandez-Baca, J. A., Ching, W. Y., Eds.; World Scientific: Singapore, 1995; p 85.

(21) Ouyang, L. Z.; Randaccio, L.; Rulis, P.; Kurmaev, E. Z.; Moewes, A.; Ching, W. Y. *J. Mol. Struct.* **2003**, *622*, 221.

(22) Ouyang, L. Z.; Rulis, P.; Ching, W. Y.; Nardin, G.; Randaccio, L. *Inorg. Chem.* **2004**, *43*, 1235.

(23) Kurmaev, E. Z.; Moewes, A.; Ouyang, L. Z.; Randaccio, L.; Rulis, P.; Ching, W. Y.; Bach, M.; Neumann, M. *Europhys. Lett.* **2003**, *62*, 582.

(24) Ouyang, L. Z.; Rulis, P.; Ching, W. Y.; Slouf, M.; Nardin, G.; Randaccio, L. *Spectrochim. Acta, Part A* **2005**, *61*, 1647.

(25) Moewes, A.; MacNaughton, J.; Wilks, R.; Lee, J. S.; Wettig, S. D.; Kraatz, H.-B.; Kurmaev, E. Z. *J. Electron Spectrosc.* **2004**, *137−40*, 817.

(26) MacNaughton, J.; Moewes, A.; Kurmaev, E. *J. Phys. Chem. B* **2005**, *109*, 7749.

(27) Bixon, M.; Jortner, J. *Adv. Chem. Phys.* **1999**, *106*, 35.

(28) van Buuren, T.; Dinh, L. N.; Chase, L. L.; Siekhaus, W. J.; Terminello, L. J. *Phys. Rev. Lett.* **1998**, *80*, 3803.

(29) Lüning, J.; Rockenberger, J.; Eisebitt, S.; Rubensson, J.-E.; Karl, A.; Kornowski, A.; Weller, H.; Eberhardt, W. *Solid State Commun.* **1999**, *112*, 5.

(30) McGuinness, C.; Fu, D.; Downes, J. E.; Smith, K. E. *J. Appl. Phys.* **2003**, *94*, 3919.

(31) Fomichev, V. A.; Rumsh, M. A. *J. Phys. Chem. Solids* **1968**, *29*, 1015.

(32) Moewes, A.; Kurmaev, E. Z.; Tse, J. S.; Geshi, M.; Ferguson, M. J.; Trofimova, V. A.; Yarmoshenko, Y. M. *Phys. Rev. B* **2002**, *65*, 153106.

(33) Taniguchi, M.; Kawai, T. *Phys. Rev. E* **2004**, *70*, 011913.